MATERIALS SCIENCE

On-chip torsion balances with femtonewton force resolution at room temperature enabled by carbon nanotube and graphene

Lin Cong[1], Zi Yuan[1], Zaiqiao Bai[2]*, Xinhe Wang[3], Wei Zhao[4], Xinyu Gao[1], Xiaopeng Hu[1,5], Peng Liu[1], Wanlin Guo[6]*, Qunqing Li[1], Shoushan Fan[1], Kaili Jiang[1,5]*

The torsion balance, consisting of a rigid balance beam suspended by a fine thread, is an ancient scientific instrument, yet it is still a very sensitive force sensor to date. As the force sensitivity is proportional to the lengths of the beam and thread, but inversely proportional to the fourth power of the diameter of the thread, nanomaterials should be ideal building blocks for torsion balances. Here, we report a torsional balance array on a chip with the highest sensitivity level enabled by using a carbon nanotube as the thread and a monolayer graphene coated with Al nanofilms as the beam and mirror. It is demonstrated that the femtonewton force exerted by a weak laser can be easily measured. The balances on the chip should serve as an ideal platform for investigating fundamental interactions up to zeptonewton in accuracy in the near future.

INTRODUCTION

The torsion balance, or more generally the torsion pendulum, is one of the most ancient scientific instruments, but it is still actively used today as a precise measuring device. It was used to discover Coulomb's law (*1*) and to determine the density of Earth (*2*) in 1785 and 1798, respectively. A detailed description of the history of the torsion balance can be found in a thorough review article by Gillies and Ritter (*3*). The instrument has played an important role in a wide variety of applications (*4*–*8*). One key focus of scientific explorations still active today is to determine the gravitational constant more precisely (*9*–*17*).

The intrinsic force sensitivity (S) of a torsion balance is proportional to the lengths of the beam (L) and suspension thread (l) but inversely proportional to the fourth power of the diameter of the thread (d) such that $S = L/2\kappa = 16Ll/\pi Gd^4$, where $\kappa = \pi Gd^4/32l$ is the torsional spring constant, which is proportional to the shear modulus (G) of the thread (*18*). Therefore, the most efficient way to achieve high sensitivity is to reduce the diameter of the suspension thread as much as possible.

In 1931, Kappler (*19*) used a centimeters-long thread, which was only a few tenths of a micrometer in diameter, to fabricate their highly sensitive torsion balance and set a record for an intrinsic force sensitivity that has never been approached. However, further reduction in diameter is limited by manufacturing and the surface properties of the materials used.

Carbon nanotubes (CNTs) have hitherto been one of the strongest and thinnest materials known (*20*, *21*). In particular, CNTs have an ultrahigh aspect ratio (*22*) conducive to being used as the torsion balance thread. Much effort has been devoted to using a CNT as the torsion spring or bearing in a nanoelectromechanical system (NEMS) device (*23*–*26*), and a CNT-based torsion pendulum has been successfully fabricated (*27*) with a measured torsional spring constant as low as 3.7×10^{-15} N·m per radian. The theoretically predicted torsional spring constant can be even smaller (*28*, *29*), down to 1.01×10^{-20} N·m per radian, which is due to the extremely small diameter of the CNT. However, the realized sensitivity remains several orders lower than the record created by Kappler.

Here, we show that with the recent advancement of synthesizing ultralong CNTs (*22*, *30*) and large-area graphene (*31*, *32*), we are now able to substantially increase the lengths of the balance beam (L) and suspension thread (l) and thus greatly improve the sensitivity to the same level as the Kappler's instrument and more than four orders of magnitude higher than other instruments in the literature. Moreover, our torsion balance is only 1% to 0.1% the size of the Kappler's device and its fabrication is compatible with the semiconductor processing such that it can be incorporated into a 4 × 4 array on a chip.

RESULTS

Design of the torsion balance

In our design, as shown in Fig. 1, an individual CNT with a diameter of a few nanometers was used as the thread to suspend the ultralight beam made of a monolayer graphene sheet coated with Al nanofilms. Each balance in the array is 300 μm × 300 μm, with a suspension length of l = 110 μm and a beam length of L = 120 μm. From the beam geometry and density of the material, it can be determined that the mass of the balance beam (m) was 8.14×10^{-13} kg, and its moment of inertia (I) was 9.76×10^{-22} kg·m^2, which is 10 orders of magnitude lower than that of Kappler's instruments (see table S1) (*19*). The extremely low moment of inertia reduces the measurement time to subseconds at room temperature, while Kappler's instrument takes hours (*19*).

Fabrication of the torsion balance array

The fabrication process of the torsion balance array is shown schematically in Fig. 2 and described in detail in Materials and Methods.

[1]State Key Laboratory of Low-Dimensional Quantum Physics, Tsinghua-Foxconn Nanotechnology Research Center, Department of Physics, Tsinghua University, Beijing 100084, China. [2]Department of Physics, Beijing Normal University, Beijing 100875, China. [3]Fert Beijing Research Institute, School of Microelectronics and Beijing Advanced Innovation Centre for Big Data and Brain Computing (BDBC), Beihang University, Beijing 100191, China. [4]No. 58th Research Institute of China Electronics Technology Research Group Corporation, Wuxi 214035, China. [5]Frontier Science Center for Quantum Information, Beijing 100084, China. [6]Key Laboratory for Intelligent Nano Materials and Devices of Ministry of Education, State Key Laboratory of Mechanics and Control of Mechanical Structures, and Institute of Nanoscience, Nanjing University of Aeronautics and Astronautics, Nanjing 210016, China.
*Corresponding author. Email: baizq@bnu.edu.cn (Z.B.); wlguo@nuaa.edu.cn (W.G.); jiangkl@tsinghua.edu.cn (K.J.)

First, we prepared a free-standing graphene-CNT film (GCF) (Fig. 2, A to C) and transferred it to a prefabricated silicon wafer with an array of 300 μm × 300 μm square through-holes (Fig. 2D). A focused laser was used to define an 80-μm-wide GCF strip as the skeleton of the mirror (Fig. 2E). We then transferred an individual CNT to the GCF-covered substrate as a suspension thread (Fig. 2F). Last, 10 nm of Al was deposited on both sides of the substrate to obtain a high-reflectivity mirror (Fig. 2G), and we removed the parts of the GCF that connect the mirror to the substrate with a laser (Fig. 2H). At this point, the mirror was able to rotate in the light field of the microscope with the CNT as the axis (see movie S1). The CNT torsion balance with a 110-μm-long CNT suspension thread and a 120 μm × 80 μm rectangular mirror was finally obtained by carefully orienting the substrate from a horizontal to vertical position (Fig. 1A). It should be mentioned that, when the substrate is turned to vertical, the lower part of CNT is slack. Only the upper part serves as the torsion thread. Thus, the CNT thread is automatically vertically aligned. Figure 2I shows a Si substrate with a 4 × 4 array of CNT torsion balances fabricated after step (Fig. 2E), one of which after step (Fig. 2H) is displayed in an optical microscope photograph in Fig. 2J. The ultrathin mirror appears to be floating in air because the CNT thread is invisible under an optical microscope.

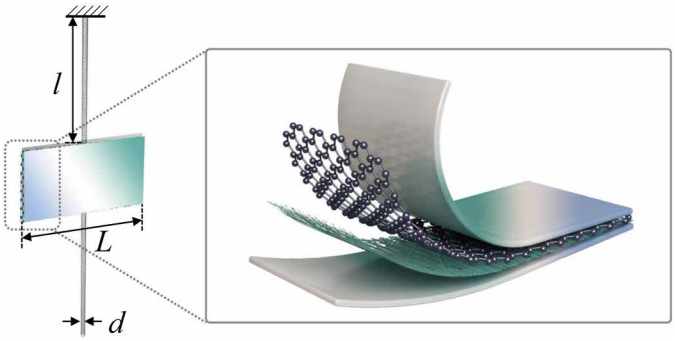

Fig. 1. Schematic illustration of the torsion balance unit. It consists of an Al/graphene/CNT/Al mirror with beam length *L* suspended by an individual CNT with diameter *d* and suspension length *l*.

Measurement and results

To eliminate the influence of air currents, the CNT torsion balance was sealed in a vacuum chamber evacuated to 10^{-6} Pa. The vacuum chamber is put on an optical workstation with Newport high-performance laminar flow isolator (S-2000 series). Thus, the vibration and mechanical noise from the environment has been isolated. When performing the measurement, the dry pump and turbo pump were stopped, and only the ion pump is working to maintain the vacuum. The optical measurement setup is illustrated in Fig. 3A (see fig. S1 for the entire apparatus). A laser beam with power of a few microwatts was focused by a 10-cm focal length lens on the

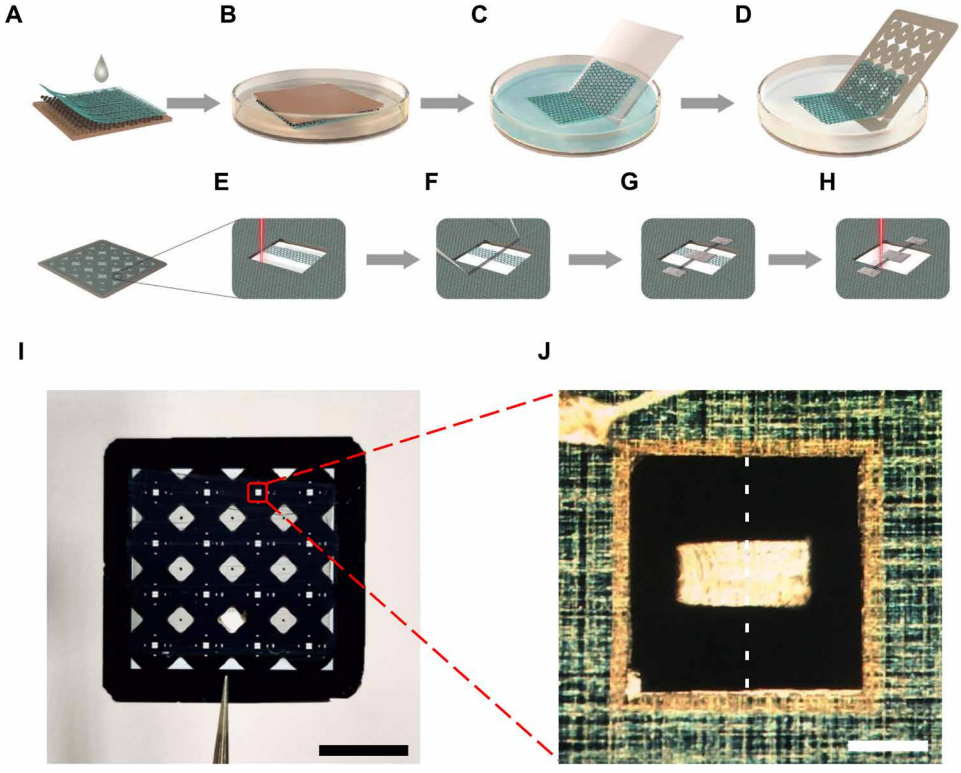

Fig. 2. The fabrication process of the CNT torsion balance. (**A**) Superaligned CNT film stuck on graphene/Cu foil after alcohol infiltration. (**B**) Inverted CNT/graphene/Cu-foil three-layer structure floating on corrosive solution. (**C**) GCF rinsed with deionized water after etching Cu away. (**D**) GCF transferred to a substrate. (**E**) Laser-trimmed GCF stripe acting as the skeleton of the mirror. (**F**) Substrate assembled with an individual CNT. (**G**) Semifinished torsion balance with 10-nm Al film deposited on both sides of the GCF stripe. (**H**) CNT torsion balance ultimately obtained by cutting off the connecting parts. (**I**) Si substrate with a 4 × 4 array of CNT torsion balances fabricated after step (E). Scale bar, 5 mm. Photo credit: Kaili Jiang, Tsinghua University. (**J**) Optical microscope photograph of a torsion balance after completing the fabrication process. The dashed line indicates the position of the CNT thread. Scale bar, 100 μm.

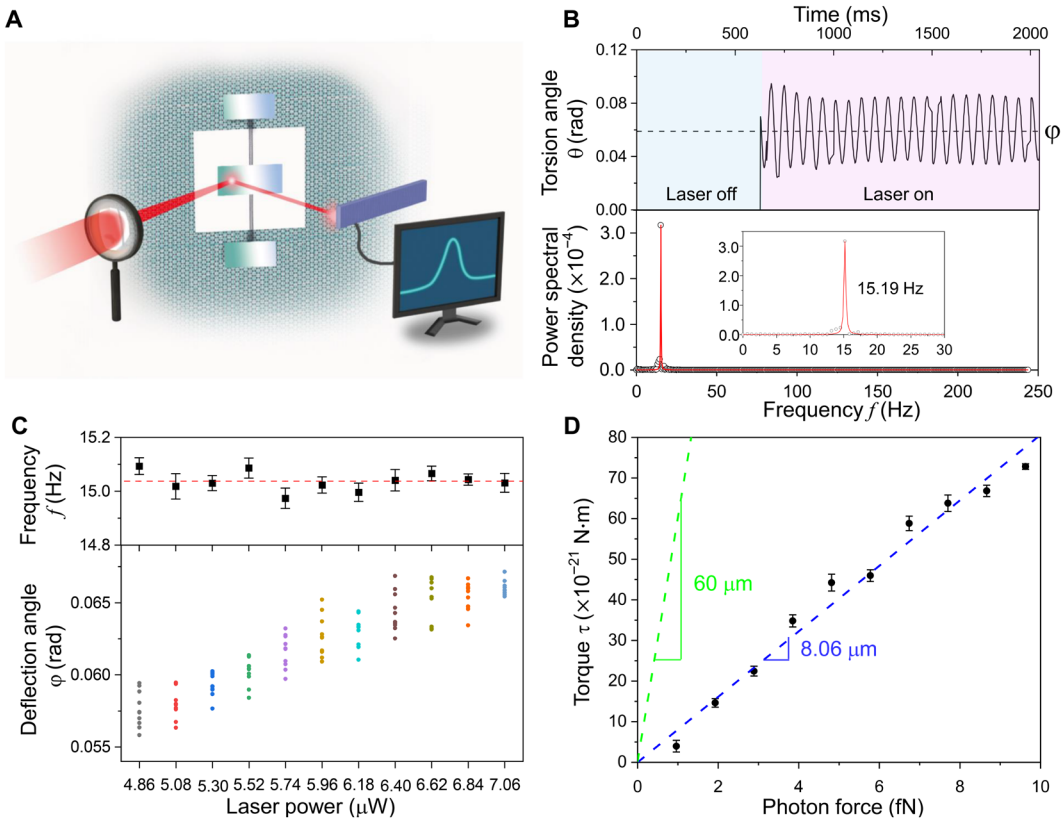

Fig. 3. The optical measurement setup and typical measurement results of CNT torsion balance #1. (**A**) Schematic diagram of the optical readout system of the torsion balance. (**B**) Dynamic response of the torsion balance to the optical pressure of a laser beam at a power of 4.86 μW (top) and the corresponding fast Fourier transform (FFT) power spectra (bottom; black circle represents the FFT data, and red line is the curve fitting). (**C**) Equilibrium deflection angles and frequency against the laser power. The error bar of the top panel is obtained from statistics on 10 independent measurements. (**D**) Torque versus incident photon force. The effective lever length in the measurement is 8.06 μm. The green dashed line is the theoretical torque-force relation at the full lever length of $L/2 = 60$ μm.

mirror to exert photon pressure that causes the torsion balance to rotate at a small angle around the CNT thread. The induced angle was measured with a line array charge-coupled device (CCD) sensor (Thorlabs LC100 Line Camera) by detecting the position of the reflected light. The line array CCD sensor, which was positioned 7 cm away from the torsion balance, comprised 2048 light-sensitive pixels (each 14 μm wide), corresponding to a deflection angle range of 0.2 rad. The angular position of the reflected light was determined by the pixel where the maximum value of the intensity distribution in the reflected light spot was located.

At room temperature, the mirror stochastically oscillates around the equilibrium position (φ), which is proportional to the photon pressure torque (τ), such that $\varphi = \tau/\kappa$. The oscillating motion was recorded by measuring the angular position (θ) of the reflected light at a sampling rate of 450 Hz. A typical result is shown in the top panel of Fig. 3B, which reads an equilibrium position of $\varphi = 0.059$ rad, an oscillating frequency of $f = 15.19$ Hz, and a period of 65.8 ms, according to the fast Fourier transform results (bottom of Fig. 3B).

Further analysis indicates that the stochastic motion of the mirror follows the Brownian motion dictated by Langevin's equation. The torsional potential energy of the mirror was measured to be slightly larger than $k_B T/2$, which is in good agreement with the theoretical value predicted by the Brownian motion theory (see details in the Supplementary Materials).

Characterization of sensitivity

To demonstrate the performance of the balance, optical readouts were conducted for 11 different laser powers ranging from 4.86 to 7.06 μW, and 10 sets of position time series were recorded at each power level and summarized in Fig. 3 (C and D). As expected, the average values of the torsional oscillation frequencies do not change with laser power (top of Fig. 3C). The overall average frequency of $f_0 = 15.04$ Hz, denoted by the red dashed line, yields the average torsional spring constant $\kappa = (2\pi f_0)^2 \cdot I = 8.72 \times 10^{-18}$ N·m per radian. The response of torque to the variation in force is illustrated in Fig. 3D, where the variation in torque is the product of the torsional spring constant, κ, and the increments in the deflection angle relative to the first group measured at 4.86 μW, Δφ. The incident photon force exerted on the mirror can be calculated by taking into consideration the factors including transmissivity of the quartz window (0.89), reflectivity of the mirror (0.69), and incident angle of the laser beam (8°) (see details in the Supplementary Materials). Because the laser spot on the mirror was too weak, the lever length could not be determined directly through an optical microscope. However, the effective lever length of the measurement could be estimated as the slope of the linear fitting equation denoted by the blue dashed line, which is 8.06 μm. The results indicated that the CNT torsion balance can measure weak force with femtonewton resolution. The deflection could be further enhanced by moving the focused laser spot to the edge of the mirror to extend the lever length to the

designed value of 60 μm. Accordingly, the laser power should be further reduced to avoid an out-of-range deflection. In this experiment, the laser was used to both measure the deflection angle and exert the weak force. Further reducing the laser power will severely affect the angle measurement. To measure sub-femtonewton force exerted by a weaker laser light, another probing laser beam should be used to detect the deflection angle.

DISCUSSION

Although various readout systems, performed optically or electrically, are used in the experiments displayed in Fig. 4, the sensitivity *S* measures the ability of the torsion balance to transduce a weak input force acting on the balance beam into a torsional angle of the suspension thread. With this definition, in most experiments, sensitivity lies between 10^5 and 10^8 rad/N, whereas it exceeded 10^{12} rad/N in Kappler's (*19*) and our works. Further comparisons of Kappler's and our torsion balances are shown in table S1. Our approach provides a reliable way to liberate the potential of the torsion balance and make it attractive for on-chip applications.

The performance of our CNT torsion balances can be further improved simply by using a small-diameter CNT as suspension thread. For example, a CNT suspension thread with a diameter of 1 nm will give rise to a torsional spring constant of 5×10^{-22} N·m per radian and a sensitivity of 10^{17} rad/N, according to the theoretical estimation (*28*, *29*). If an interferometer is adopted to detect the small displacement of the mirror, the force of a zeptonewton (10^{-21} N) can be measured precisely at room temperature. The expected zeptonewton force resolution would break the record of hundreds of zeptonewtons obtained at ultralow temperature (*33*, *34*) and make an important breakthrough in the field of weak force measurement. As the torsion angle of the CNT is continuously adjustable by tuning light intensity, the influence on the electron transport properties and band structure produced by torsional strain can also be explored over a wider range (*26*, *35*, *36*) using the CNT torsion balance.

The 4 × 4 array on the chip also offers new opportunities to extend the dynamical range of weak force measurement by selecting CNTs with different diameters for the 16 torsion balances. For diameters ranging from 1 to 10 nm, the torsion balance in the current design gives rise to sensitivities ranging from 10^{13} to 10^{17} rad/N, corresponding to ranges of force measurement from 2×10^{-14} to 2×10^{-18} N. This wide dynamical range will enable a diverse spectrum of applications in weak force measurement.

However, the current study is quite preliminary. There are many aspects that need to be further improved, among which the following two are imperative: (i) A transmission electron microscopy (TEM) window should be incorporated into the chip to get the information of the CNT such as diameter and chiral index; (ii) the measurement of the deflection angle and exertion of weak force should be decoupled so that reducing the applied force will not affect the measurement of the deflection angle.

In conclusion, we have developed on-chip CNT torsion balances with femtonewton resolution by using an individual CNT as the suspension thread and an aluminized GCF as the balance beam and mirror. The CNT torsion balance measures forces 10,000 times faster than Kappler's instrument, with similar sensitivity that is more than four orders of magnitude higher than other instruments in the literature. The high sensitivity and simple fabrication of the CNT torsion balance enable new fundamental research and further applications, such as exploring weak effects and discovering new physics laws.

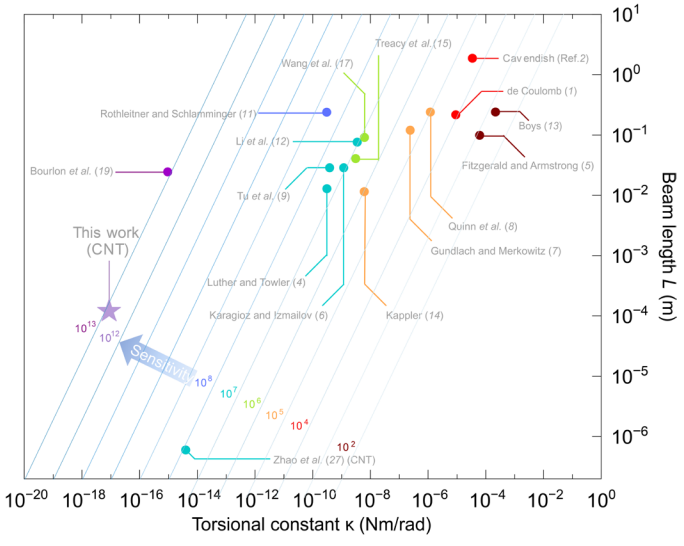

Fig. 4. The comparison map of CNT torsion balances and classical torsion balances. In addition to displaying the measured torsional constant κ and beam length *L* of each experiment, the sensitivity of the apparatus defined by the deflection angle produced by 1 N is also shown, which can be obtained from *L*/2κ. The parallel lines colored from light blue to dark blue indicate orders of magnitude of sensitivity ranging from 2 to 13. The experiments are grouped and separated by color according to the order of magnitude of sensitivity.

MATERIALS AND METHODS

Preparation of GCFs

Large-area, continuous polycrystalline graphene was synthesized on commercially available Cu foils (25 μm thick; 99.8%, Alfa Aesar) in a low-pressure chemical vapor deposition system equipped with a quartz tube 2.54 cm in diameter. The growth parameters were similar to those in literature (*32*): At 13 Pa, the system was heated with H_2 [5 standard cubic centimeter per minute (sccm)] to 1040°C for 40 min followed by annealing for 30 min; CH_4 (30 sccm) was introduced as a carbon source at 66 Pa for 20 min, and last, the system was cooled down naturally with H_2 (5 sccm) and CH_4 (30 sccm). Reactive ion etching (RIE) treatment (40 sccm O_2, 10 Pa, 20 W, 10 s) was used to remove graphene on one side of the Cu foil, and two layers of super-aligned CNT (SACNT) films were cross-stacked on the other side followed by the alcohol treatment. The CNT/graphene/Cu three-layer structure was inverted and floated on $(NH_4)_2S_2O_8$ solution (0.1 M) to etch the Cu foil, leaving a GCF sample floating on the surface of the corrosive solution.

Growth of CNTs

The ultralong CNTs were grown on a Si substrate with trenches 500 μm wide. The furnace was heated to 950°C in an atmosphere of H_2 (500 sccm) and CH_4 (200 sccm) followed by a growing process in H_2 (5 sccm) and CH_4 (2 sccm) for 4 min. The sample was then cooled down to room temperature within 8 min in an atmosphere of Ar (1000 sccm).

Fabrication of the torsion balance array

The fabrication process of the torsion balance array is shown schematically in Fig. 2. Two layers of SACNT films (*37*, *38*) were

cross-stacked on chemical vapor–deposited monolayer graphene/Cu foil. To prepare the final flat mirror surface, graphene on the other side of the Cu foil was removed by oxygen RIE. The CNT network was tightly attached to the graphene after alcohol treatment (Fig. 2A) (*31*). The three-layer structure was inverted and kept afloat on the surface of the corrosive solution [0.1 M $(NH_4)_2S_2O_8$] with the CNT network on the bottom (Fig. 2B). After etching the Cu foil away, the free-standing GCF with a glass slide was rinsed with deionized water three times (Fig. 2C). The GCF was transferred to a prefabricated Si wafer with an array of 300 μm × 300 μm square through-holes (Fig. 2D). The upper and lower parts of the suspended square GCF were cut off with a focused laser, leaving the middle 80-μm-wide GCF strip as the skeleton of mirror (Fig. 2E). An individual CNT grown by chemical vapor deposition (*22*) was transferred to the GCF-covered substrate, with the CNT coinciding with the perpendicular bisector of the strip film as the suspension thread (Fig. 2F). Al (10 nm thick) was deposited on both sides of the substrate to obtain a highly reflective surface, and the two ends of the CNT were fixed (Fig. 2G). The parts of GCF that connected the mirror to the substrate were removed with a laser (Fig. 2H). At that point, the mirror was able to rotate in the light field of the microscope with the CNT as the axis (see movie S1). The CNT torsion balance with a 110-μm-long CNT suspension thread and a 120 μm × 80 μm rectangular mirror was finally obtained by carefully positioning the substrate from a horizontal to vertical orientation (Fig. 1A).

Transfer an individual CNT onto GCF

The ultralong CNTs were grown over a trench 500 μm wide on a silicon substrate. The substrate with ultralong CNTs was then put on top of a quartz crucible, which was loaded with some sulfur and heated to 120°C by a hot plate, for approximately 10 s. The ultralong CNTs were therefore decorated with sulfur nanoparticles, which scatter light and make CNT visible under an optical microscope (*39*). Then, the CNTs were transferred to a predefined position on the GCF by using a homemade micromanipulator under an optical microscope. By heating the substrate to 120°C for 1 min, the decorated sulfur nanoparticles can be totally removed.

Depositing Al nanofilm

An e-beam evaporation system (Anelva L-400EK) was used to deposit the Al nanofilm (10 nm thick at 0.5 Å/s) on GCF through a shadow mask to avoid depositing Al on suspending CNTs. The thickness was measured in situ by using a quartz crystal sensor, which was calibrated by using an atomic force microscope (AFM; Veeco Dimension V). According to Tavernarakis *et al.* (*40*), if CNT is decorated by metal nanoparticles, it might be visible in an optical microscope. However, the CNT suspension thread of the torsion balance is invisible in optical microscope. There might be some Al deposition on the part adjacent to GCF, but the other parts of suspended CNT are free of Al deposition according to the scanning electron microscopy (SEM) images.

Prepare SACNT film

The SACNT film can be directly drawn out from a SACNT array, which is synthesized in low-pressure chemical vapor deposition (CVD) furnaces at a temperature of 700°C by using acetylene as precursor. Details can be found in (*38*).

Laser cutting

A supercontinuum white laser (NKT SuperK Compact; nanosecond laser pulse at a 20-kHz repetition rate, 110 mW) passed through a long–working distance 50× objective and was focused into a micrometer-sized spot to cut the GCFs with/without Al film.

SUPPLEMENTARY MATERIALS

Supplementary material for this article is available at http://advances.sciencemag.org/cgi/content/full/7/12/eabd2358/DC1

REFERENCES AND NOTES

1. C. A. de Coulomb, Premier Mémoire sur l'Electricité et le Magnétisme. *Mém. Acad. Roy. Sci.*, 569–577 (1785).
2. H. Cavendish, XXI. Experiments to determine the density of the earth. *Philos. Trans. R. Soc. B* **88**, 469–526 (1798).
3. G. T. Gillies, R. C. Ritter, Torsion balances, torsion pendulums, and related devices. *Rev. Sci. Instrum.* **64**, 283–309 (1993).
4. E. F. Nichols, G. F. Hull, A preliminary communication on the pressure of heat and light radiation. *Phys. Rev. (Series I)* **13**, 307–320 (1901).
5. G. I. González, P. R. Saulson, Brownian motion of a torsion pendulum with internal friction. *Phys. Lett. A* **201**, 12–18 (1995).
6. C. H. Bagley, G. G. Luther, Preliminary results of a determination of the newtonian constant of gravitation: A test of the kuroda hypothesis. *Phys. Rev. Lett.* **78**, 3047–3050 (1997).
7. S. Matsumura, N. Kanda, T. Tomaru, H. Ishizuka, K. Kuroda, A measurement of the frequency dependence of the spring constant. *Phys. Lett. A* **244**, 4–8 (1998).
8. J. Luo, L.-C. Tu, Z.-K. Hu, E.-J. Luan, New experimental limit on the photon rest mass with a rotating torsion balance. *Phys. Rev. Lett.* **90**, 081801 (2003).
9. G. G. Luther, W. R. Towler, Redetermination of the Newtonian gravitational constant *G*. *Phys. Rev. Lett.* **48**, 121–123 (1982).
10. M. P. Fitzgerald, T. R. Armstrong, Newton's gravitational constant with uncertainty less than 100 ppm. *IEEE Trans. Instrum. Meas.* **44**, 494–497 (1995).
11. O. V. Karagioz, V. P. Izmailov, Measurement of the gravitational constant with a torsion balance. *Meas. Tech.* **39**, 979–987 (1996).
12. J. H. Gundlach, S. M. Merkowitz, Measurement of Newton's constant using a torsion balance with angular acceleration feedback. *Phys. Rev. Lett.* **85**, 2869–2872 (2000).
13. T. J. Quinn, C. C. Speake, S. J. Richman, R. S. Davis, A. Picard, A new determination of G using two methods. *Phys. Rev. Lett.* **87**, 111101 (2001).
14. L. C. Tu, Q. Li, Q. L. Wang, C. G. Shao, S. Q. Yang, L. X. Liu, Q. Liu, J. Luo, New determination of the gravitational constant G with time-of-swing method. *Phys. Rev. D* **82**, 022001 (2010).
15. R. Newman, M. Bantel, E. Berg, W. Cross, A measurement of *G* with a cryogenic torsion pendulum. *Philos. Trans. R. Soc. A* **372**, 20140025 (2014).
16. C. Rothleitner, S. Schlamminger, Invited review article: Measurements of the Newtonian constant of gravitation, G. *G. Rev. Sci. Instrum.* **88**, 111101 (2017).
17. Q. Li, C. Xue, J. P. Liu, J. F. Wu, S. Q. Yang, C. G. Shao, L. D. Quan, W. H. Tan, L. C. Tu, Q. Liu, H. Xu, L. X. Liu, Q. L. Wang, Z. K. Hu, Z. B. Zhou, P. S. Luo, S. C. Wu, V. Milyukov, J. Luo, Measurements of the gravitational constant using two independent methods. *Nature* **560**, 582–588 (2018).
18. C. V. I. Boys, On the Newtonian constant of gravitation. *Philos. Trans. R. Soc. London A* **186**, 1–72 (1895).
19. E. Kappler, Versuche zur Messung der Avogadro-Loschmidtschen Zahl aus der Brownschen Bewegung einer Drehwaage. *Ann. Phys.* **403**, 233–256 (1931).
20. M. M. J. Treacy, T. W. Ebbesen, J. M. Gibson, Exceptionally high Young's modulus observed for individual carbon nanotubes. *Nature* **381**, 678–680 (1996).
21. J. P. Lu, Elastic properties of carbon nanotubes and nanoropes. *Phys. Rev. Lett.* **79**, 4 (1997).
22. X. Wang, Q. Li, J. Xie, Z. Jin, J. Wang, Y. Li, K. Jiang, S. Fan, Fabrication of ultralong and electrically uniform single-walled carbon nanotubes on clean substrates. *Nano Lett.* **9**, 3137–3141 (2009).
23. P. A. Williams, S. J. Papadakis, A. M. Patel, M. R. Falvo, S. Washburn, R. Superfine, Fabrication of nanometer-scale mechanical devices incorporating individual multiwalled carbon nanotubes as torsional springs. *Appl. Phys. Lett.* **82**, 805–807 (2003).
24. B. Bourlon, D. C. Glattli, C. Miko, L. Forró, A. Bachtold, Carbon nanotube based bearing for rotational motions. *Nano Lett.* **4**, 709–712 (2004).
25. A. M. Fennimore, T. D. Yuzvinsky, W. Q. Han, M. S. Fuhrer, J. Cumings, A. Zettl, Rotational actuators based on carbon nanotubes. *Nature* **424**, 408–410 (2003).
26. T. Cohen-Karni, L. Segev, O. Srur-Lavi, S. R. Cohen, E. Joselevich, Torsional electromechanical quantum oscillations in carbon nanotubes. *Nat. Nanotechnol.* **1**, 36–41 (2006).

27. S. J. Papadakis, A. R. Hall, P. A. Williams, L. Vicci, M. R. Falvo, R. Superfine, S. Washburn, Resonant oscillators with carbon-nanotube torsion springs. *Phys. Rev. Lett.* **93**, 146101 (2004).
28. J. C. Meyer, M. Paillet, S. Roth, Single-molecule torsional pendulum. *Science* **309**, 1539–1541 (2005).
29. B. Shen, Z. Zhu, J. Zhang, H. Xie, Y. Bai, F. Wei, Single-carbon-nanotube manipulations and devices based on macroscale anthracene flakes. *Adv. Mater.* **30**, 1705844 (2018).
30. R. Zhang, Y. Zhang, Q. Zhang, H. Xie, W. Qian, F. Wei, Growth of half-meter long carbon nanotubes based on Schulz–Flory distribution. *ACS Nano* **7**, 6156–6161 (2013).
31. X. Lin, P. Liu, Y. Wei, Q. Li, J. Wang, Y. Wu, C. Feng, L. Zhang, S. Fan, K. Jiang, Development of an ultra-thin film comprised of a graphene membrane and carbon nanotube vein support. *Nat. Commun.* **4**, 2920 (2013).
32. W. Zhao, B. Xia, L. Lin, X. Xiao, P. Liu, X. Lin, H. Peng, Y. Zhu, R. Yu, P. Lei, J. Wang, L. Zhang, Y. Xu, M. Zhao, L. Peng, Q. Li, W. Duan, Z. Liu, S. Fan, K. Jiang, Low-energy transmission electron diffraction and imaging of large-area graphene. *Sci. Adv.* **3**, e1603231 (2017).
33. V. Blūms, M. Piotrowski, M. I. Hussain, B. G. Norton, S. C. Connell, S. Gensemer, M. Lobino, E. W. Streed, A single-atom 3D sub-attonewton force sensor. *Sci. Adv.* **4**, eaao4453 (2018).
34. M. Héritier, A. Eichler, Y. Pan, U. Grob, I. Shorubalko, M. D. Krass, Y. Tao, C. L. Degen, Nanoladder cantilevers made from diamond and silicon. *Nano Lett.* **18**, 1814–1818 (2018).
35. A. R. Hall, M. R. Falvo, R. Superfine, S. Washburn, Electromechanical response of single-walled carbon nanotubes to torsional strain in a self-contained device. *Nat. Nanotechnol.* **2**, 413–416 (2007).
36. K. S. Nagapriya, S. Berber, T. Cohen-Karni, L. Segev, O. Srur-Lavi, D. Tománek, E. Joselevich, Origin of torsion-induced conductance oscillations in carbon nanotubes. *Phys. Rev. B* **78**, 165417 (2008).
37. K. Jiang, Q. Li, S. Fan, Spinning continuous carbon nanotube yarns. *Nature* **419**, 801 (2002).
38. K. Jiang, J. Wang, Q. Li, L. Liu, C. Liu, S. Fan, Superaligned carbon nanotube arrays, films, and yarns: A road to applications. *Adv. Mater.* **23**, 1154–1161 (2011).
39. M. Jian, H. Xie, Q. Wang, K. Xia, Z. Yin, M. Zhang, N. Deng, L. Wang, T. Ren, Y. Zhang, Volatile-nanoparticle-assisted optical visualization of individual carbon nanotubes and other nanomaterials. *Nanoscale* **8**, 13437–13444 (2016).
40. A. Tavernarakis, A. Stavrinadis, A. Nowak, I. Tsioutsios, A. Bachtold, P. Verlot, Optomechanics with a hybrid carbon nanotube resonator. *Nat. Commun.* **9**, 662 (2018).
41. A. Einstein, Zur Theorie der Brownschen Bewegung. *Ann. Phys.* **324**, 371–381 (1906).
42. M. Von Smoluchowski, Zur kinetischen theorie der brownschen molekularbewegung und der suspensionen. *Ann. Phys.* **326**, 756–780 (1906).
43. P. Langevin, Sur la théorie du mouvement brownien. *Compt. Rendus* **146**, 530 (1908).
44. A. D. Fokker, Die mittlere Energie rotierender elektrischer Dipole im Strahlungsfeld. *Ann. Phys.* **348**, 810–820 (1914).
45. M. Planck, *Uber einen Satz der statistichen Dynamik und eine Erweiterung in der Quantumtheorie* (Preuss. Akad. Wiss, 1917).
46. R. M. Mazo, *Brownian Motion: Fluctuations, Dynamics, and Applications* (Oxford Univ. Press on Demand, 2002).
47. M. V. Smoluchowski, Über Brownsche Molekularbewegung unter Einwirkung äußerer Kräfte und deren Zusammenhang mit der verallgemeinerten Diffusionsgleichung. *Ann. Phys.* **353**, 1103–1112 (1916).
48. W. Gerlach, E. Lehrer, Über die Messung der rotatorischen Brownschen Bewegung mit Hilfe einer Drehwage. *Naturwissenschaften* **15**, 15 (1927).
49. C. R. Rao, Information and the accuracy attainable in the estimation of statistical parameters. *Bull. Calcutta Math. Soc.* **37**, 81–89 (1945).
50. H. Cramér, *Mathematical Methods of Statistics* (Princeton Univ. Press, 1946).
51. L. Haiberger, M. Weingran, S. Schiller, Highly sensitive silicon crystal torque sensor operating at the thermal noise limit. *Rev. Sci. Instrum.* **78**, 025101 (2007).
52. J. Moser, J. Güttinger, A. Eichler, M. J. Esplandiu, D. E. Liu, M. I. Dykman, A. Bachtold, Ultrasensitive force detection with a nanotube mechanical resonator. *Nat. Nanotechnol.* **8**, 493–496 (2013).
53. P. Weber, H. L. Calvo, J. Bohle, K. Goß, C. Meyer, M. R. Wegewijs, C. Stampfer, Switchable coupling of vibrations to two-electron carbon-nanotube quantum dot states. *Nano Lett.* **15**, 4417–4422 (2015).
54. P. Weber, J. Güttinger, A. Noury, J. Vergara-Cruz, A. Bachtold, Force sensitivity of multilayer graphene optomechanical devices. *Nat. Commun.* **7**, 12496 (2016).

Acknowledgments

Funding: This work is financially supported by the NSFC (51727805 and 51788104), the National Key Research and Development Program of China (2018YFA0208400), and the Beijing Advanced Innovation Center for Future Chips (ICFC). **Author contributions:** L.C. and K.J. proposed and designed the research. L.C., Z.Y., X.W., X.H., P.L., and K.J. contributed to the experimental setup. W.Z. provided graphene. X.G. grew ultralong CNTs. L.C. performed the CNT torsion balance fabrication and photon pressure measurements. L.C., Z.Y., and Z.B. contributed to data processing. L.C. and Z.B. contributed to the theoretical analysis. L.C., Z.B., W.G., and K.J. wrote the paper. Q.L. and S.F. provided the facilities for microfabrication. All the authors participated in the research discussion. **Competing interests:** L.C., Z.Y., K.J., and S.F. are inventors on a patent application related to this work filed by Tsinghua University and Hon Hai Precision Industry Co. Ltd. (no. 17/147769, filed on 13 January 2021). L.C., Z.Y., K.J., and S.F. are also inventors on a patent application related to this work filed by Tsinghua University and Hon Hai Precision Industry Co. Ltd. (no. 17/147767, filed on 13 January 2021). The authors declare no other competing interests. **Data and materials availability:** All data needed to evaluate the conclusions in the paper are present in the paper and/or the Supplementary Materials. Additional data related to this paper may be requested from the authors.

Submitted 9 June 2020
Accepted 29 January 2021
Published 17 March 2021
10.1126/sciadv.abd2358

Citation: L. Cong, Z. Yuan, Z. Bai, X. Wang, W. Zhao, X. Gao, X. Hu, P. Liu, W. Guo, Q. Li, S. Fan, K. Jiang, On-chip torsion balances with femtonewton force resolution at room temperature enabled by carbon nanotube and graphene. *Sci. Adv.* **7**, eabd2358 (2021).